Effect of Interfacial Curvature on the Miscibility of Laterally Mobile, Mixed Polyelectrolyte and Neutral Polymer Brushes: An SCF Numerical Analysis

Kevin N. Witte and You-Yeon Won*

School of Chemical Engineering, Purdue University, West Lafayette, Indiana 47907

Received July 27, 2007
Revised Manuscript Received January 17, 2008

Introduction

Polymer chains with one end grafted to an interface at high enough density to form a brush configuration have been extensively studied,[1–4] with recent efforts focused on brushes tethered to curved interfaces. These theoretical systems more closely model self-assembled polymer structures and polymer-stabilized colloids.[5–14] Significant attention has been devoted to mixed brushes containing (at least) two chemically distinct polymers grafted to planar surfaces.[15–17] However, mixed brushes on curved surfaces have received less attention, but it has been shown that self-assembled polymer structures containing polyelectrolytes are more favorable when consisting of curved surfaces.[18,19] Mixed brushes, besides being technically relevant for mixed/multicomponent block copolymer self-assembly and the creation of responsive surfaces,[20] can exhibit interesting phase segregation behavior on various length scales. Brushes with fixed grafting points show many unique molecular-scale phase separations both along the direction perpendicular and in the plane of the grafting surface.[20–23] Polymers with mobile grafting points, such as block copolymer assemblies at the air–water interface or in vesicles and micelles, can show macroscopic phase separation.[24,25] Recently, we studied, using SCF theory, mixtures of incompatible polyelectrolyte and neutral polymer brushes with mobile grafting points in a flat geometry as might be encountered at an infinite air–water interface.[26] The mixed brushes favor a phase-separated state along the interface as the grafting density is increased due to a larger contribution from the polymer–polymer excluded-volume cross-interaction which is dependent upon segment proximity. However, increasing the effective charge on the polyelectrolyte chains favors mixing due to a charge dilution associated with the mixed state. This observation is in strong agreement with the literature on homopolymer and diblock copolymer mixtures.[27,28] In the present paper, we examine the effect of grafting surface curvature on these laterally mobile mixtures of polyelectrolyte and uncharged polymer brushes (Scheme 1). Specifically, the miscibility of two chemically incompatible polymer species is studied as a function of the surface mean curvature in two different interfacial geometries: spherical and cylindrical. The SCF equations for a mixture of polyelectrolyte and neutral polymer brushes[26] were one-dimensionalized in curvilinear coordinate systems and solved numerically. The one-dimensionalized version of the free energy of mixing formalism was analyzed to determine brush miscibility as a function of surface curvature.

Self-Consistent-Field Theory

We have shown that, for a system of polyelectrolyte and uncharged polymer brushes with added salt, the mean-field free energy can be written as[26]

$$\beta F = \int \mathrm{d}\mathbf{r} \left(\frac{1}{2}\beta\varepsilon|\nabla\psi(\mathbf{r})|^2 - \sum_P \sum_{P'} \frac{1}{2} v_{PP'}\rho_P(\mathbf{r})\rho_{P'}(\mathbf{r}) - \sum_M (\rho_M(\mathbf{r}) - c_M) \right) - \sum_P n_P \ln\left[\int \mathrm{d}\mathbf{R}' \int \mathrm{d}\mathbf{R}'' \, G_P(\mathbf{R}'',\mathbf{R}',N_P) \right] + \sum_P n_P[\ln(n_P) - 1] + \sum_M c_M V[\ln(c_M V) - 1] \quad (1)$$

where β is the inverse thermal energy, ε is the dielectric constant of the system, $\Psi(\mathbf{r})$ is the dimensionless electrostatic potential, $\rho_P(\mathbf{r})$ is the segment density of a polymer of type P (denoted A and C for neutral and charged chains, respectively), $v_{PP'}$ is the excluded-volume parameter describing the interactions between polymers of types P and P', $\rho_M(\mathbf{r})$ is the density of a small ion of type M, c_M is the bulk number density of small ions, n_P is the number of polymer chains of type P, $G_P(\mathbf{R}'', \mathbf{R}', s)$ is the Green function which gives the probability density of finding a segment of polymer type P at a point $\mathbf{R}''$ after s steps along the chain beginning at the point $\mathbf{R}'$, and V is the system volume. The density fields, electric potential, and Green functions can be calculated from a set of self-consistent equations

$$\rho_P(\mathbf{r}) = \frac{\sum_i^{n_P} \int \mathrm{d}s \int \mathrm{d}\mathbf{R}' \int \mathrm{d}\mathbf{R}'' \, G_{Pi}(\mathbf{r},\mathbf{R}', s) \, G_{Pi}(\mathbf{R}'',\mathbf{r},N_P - s)}{\int \mathrm{d}\mathbf{R}' \int \mathrm{d}\mathbf{R}'' \, G_P(\mathbf{R}'',\mathbf{R}',N_P)} \quad (2)$$

$$\rho_M(\mathbf{r}) = c_M \exp(-z_M\psi(\mathbf{r})) \quad (3)$$

$$\nabla^2\psi(\mathbf{r}) = -l_B\left(\sum_P z_P f \rho_P(\mathbf{r}) + \sum_M z_M \rho_M(\mathbf{r}) \right) \quad (4)$$

$$\frac{\partial G_P(\mathbf{r},\mathbf{r}',s)}{\partial s} - \frac{b^2}{6}\nabla^2 G_P(\mathbf{r}, \mathbf{r}', s) + U_{ex}(\mathbf{r}) \, G_P(\mathbf{r},\mathbf{r}', s) = \delta(\mathbf{r} - \mathbf{r}') \, \delta(s) \quad (5)$$

$$U_{ex}(\mathbf{r}) = v_{PP}\rho_P(\mathbf{r}) + v_{PP'}\rho_{P'}(\mathbf{r}) + z_P f \psi(\mathbf{r}) \quad (6)$$

where N_P is the number of monomer segments in a polymer chain of type P, z_M is the valency of the small ion, l_B is the Bjerrum length, z_P is the valency of the polyelectrolyte segment, f is the "smeared" charge fraction per polyelectrolyte segment, b is the Kuhn length of the monomer, and U_{ex} is the external potential field with which the polymer segment is interacting. This field takes the form given in eq 6 for the case of a mixture of polyelectrolyte and neutral polymer brushes.

For solving eq 4 the following boundary conditions are used; the electric field is zero at the grafting surface ($\nabla\Psi|_{surface} = 0$), and the electrostatic potential is zero in the bulk ($\Psi|_{bulk} \rightarrow 0$) which imposes charge neutrality. This latter condition requires that $\sum_M z_M c_M = 0$ for an electrically neutral polyelectrolyte brush system with infinite size. Thus, these equations are limited

* To whom correspondence should be addressed. E-mail: yywon@ecn.purdue.edu.

10.1021/ma071682e CCC: $40.75
Published on Web 02/21/2008

Scheme 1. Illustration of Mixed (Left) and Unmixed (Right) States for Uncharged and Polyelectrolyte Polymer Brushes Grafted to Curved Interfaces with Mobile Grafting Points

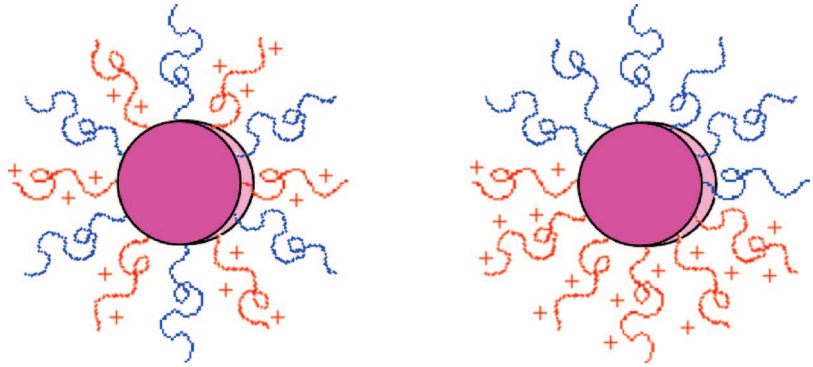

to systems containing added salt, not just counterions. In eq 5, the delta functions on the right-hand side represent the initial condition used to solve the partial differential equation. The boundary conditions for the Green function are a nonadsorbing surface ($G|_{\text{surface}} = 0$) and the fact that no monomers can exist farther from the surface than the full contour length of a chain perpendicular to the surface ($G|_{\text{contour length}} = 0$). Employing the standard volume elements and Laplacian operators, the SCF equations can be formulated in both cylindrical and spherical coordinate systems. Assuming that the grafting density is sufficiently high to form a brush structure and any mixed states are thermally averaged, the variation in the system occurs only in the radial direction. Thus, the equations can be made one-dimensional and are readily solved. The binary free energy of mixing, as a function of the composition of polyelectrolyte chains, x_C, can be calculated in the standard way as

$$\Delta F_{\text{mix}} = F(x_C) - x_C F(x_C = 1) - (1 - x_C)F(x_C = 0) \qquad (7)$$

By analyzing the free energy of mixing, spinodal and binodal curves for phase separation can be constructed by varying a system parameter, such as surface radius, and calculating the compositional limits of stability. Recall that the free energy of mixing formalism does not say anything about the nature of any "phase separation"; rather, it states when the thermally averaged (in all directions except radially) mixture is thermodynamically unstable. See ref 26 for a detailed description of the numerical process.

Results and Discussion

The miscibility of the mixed brush system is governed by a balance between like-chain and unlike-chain interactions; cross-interactions between unlike chains in an incompatible mixture (i.e., repulsion between different types of chains) drives phase separation, whereas self-interactions (like-chain repulsion of electrostatic and/or osmotic origin) drive phase mixing. Increasing surface curvature will reduce both of these driving forces for phase separation and mixing due to dilution of space. In the high salt concentration limit, the net effect of increasing the curvature will be determined predominantly by which one of the two types of interactions (i.e., self- vs cross-interactions) is dominant and can be considered in terms of the onset of mixture instability. Figure 1 shows a plot of the critical value of the cross excluded-volume parameter, υ_{AC}, against the critical charge fraction for low (≈0) curvature (solid curve) where the chain length is $N = 50$, the Kuhn length is $b = 7$ Å, the grafting density is $\sigma = 0.01$ Å^{-2}, the added salt concentration is $c_M =$ 150 mM, and the excluded-volume parameters are $\upsilon_{AA} = 125$ Å^3 and $\upsilon_{CC} = 35$ Å^3. Under these conditions the average chain-to-chain separation is roughly half the radius of gyration; hence, the configurations represent a true polymer brush. This plot was constructed by noting what value, in flat geometry (the radius of curvature (R) was set at 5×10^7 Å for these calculations), of υ_{AC} caused a change in curvature of ΔF_{mix} at constant values of f. See the Supporting Information for representative examples of the free energy of mixing plots. Also shown in the figure for comparison is the phase separation boundary for the case of curved spherical ($R = 50$ Å) interfacial geometry (broken curve). In either case, above the phase separation boundary, the mixed brush system becomes phase separated, and below the curve, the system is in the mixed state.

To confirm that the above (mixture instability) criterion is capable of predicting the exact conditions for the switching of the trend in the effect of curvature, the parameter space is probed by systematically varying f and υ_{AC} and examining the ΔF_{mix} vs x_C profile at high and low curvatures to determine which case showed higher miscibility which is defined to be the system

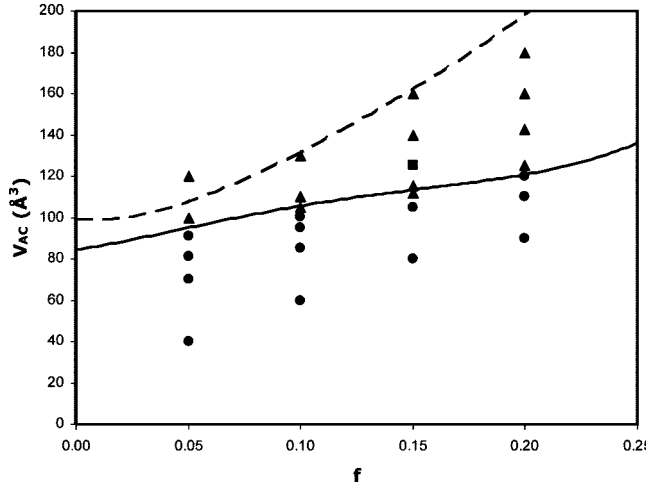

Figure 1. Plot of critical cross excluded-volume parameter, υ_{AC}, as a function of smeared charge fraction, f, for chains of $N = 50$, Kuhn length $b = 7$ Å, grafting density $\sigma = 0.01$ Å^{-2}, excluded-volume interaction $\upsilon_{AA} = 125$ Å^3, and $\upsilon_{CC} = 35$ Å^3. The solid and broken curves respectively represent the phase separation boundaries for the cases of flat ($R = 5 \times 10^7$ Å) and curved spherical ($R = 50$ Å) interfacial geometries; above the respective curve, the system becomes phase separated, and below the curve, the system is in the mixed state. The bulk salt concentration is $c_M = 150$ mM. The parameter values used to test the effect of surface curvature on the miscibility of the brushes are indicated: (▲) showed increased miscibility with increasing curvature (from $R = 5 \times 10^7$ to 50 Å), (●) showed decreased miscibility with increasing curvature (from $R = 5 \times 10^7$ to 50 Å), and (■) location of constructed composition−mean curvature phase diagram (shown in Figure 2).

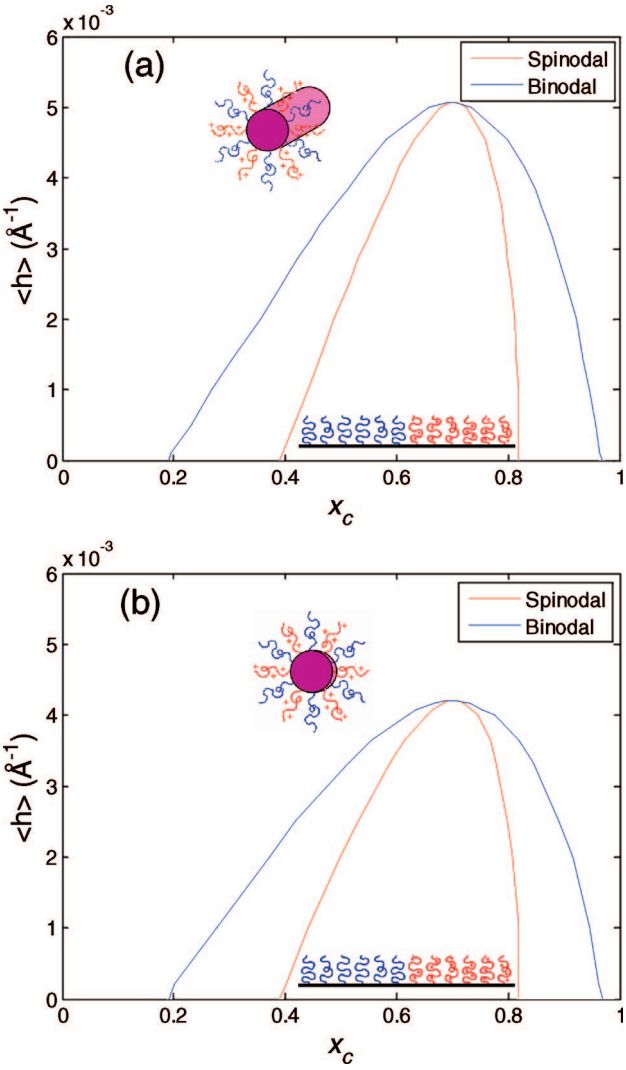

Figure 2. Phase diagram in (a) cylindrical and (b) spherical coordinates illustrating increased miscibility with increasing mean curvature $\langle h \rangle$ as a function of polyelectrolyte composition x_C for chains of length $N = 50$, Kuhn length $b = 7$ Å, grafting density $\sigma = 0.01$ Å^{-2}, excluded-volume interaction $v_{AA} = 125$ Å^3, $v_{AC} = 125$ Å^3, $v_{CC} = 35$ Å^3, and charge fractions on the polyelectrolyte chains $f = 0.15$. The bulk salt concentration is $c_M = 150$ mM.

with the more negative free energy change of mixing that does not show any region of thermodynamic instability. In the demixing dominant region, which appears above the large radius curve, the polymer–polymer cross excluded-volume parameter dominates. Curving the grafting surface dilutes space as a function of radial position, thus decreasing the strength of this interaction which is highly dependent upon the relative proximity of the monomer types. In all cases probed (the points denoted with triangles in Figure 1), the two chain types were found to be more miscible at higher curvatures because below the small radius curve, mixture instability does not occur at high curvature. Even in the region where demixing occurs at low curvature, above the small radius curve, the phase envelope is much wider at low curvature, indicating greater instability. To further illustrate the effect of surface curvature on the miscibility of the mixed brushes in the excluded-volume dominant regime, the point $f = 0.15$ and $v_{AC} = 125$ Å^3 is chosen (see Figure 1) for construction of phase diagrams. Plots of binodal and spinodal compositions calculated for this condition as functions of the mean curvature, $\langle h \rangle$, of the grafting surface for cylindrical and spherical mixed brushes are shown in Figure 2. The system shows phase separation at zero curvature, and increasing the surface curvature reduces the driving force for phase separation, eventually leading to the closure of the two-phase envelope.

In the mixing dominant region, which appears below the large radius curve in Figure 1, the positive like-chain excluded volumes and electrostatics dominate. These interactions favor a mixed brush state, and they also weaken as the space is diluted due to an increase in the curvature of the grafting surface. Since these terms dominate the interactions, reducing their strength reduces the overall favorability of the mixture. Thus, if phase separation were to occur in this regime, it would be possible to see a lower critical curvature value. The parameter space for spherical geometry is systematically explored attempting to find this type of behavior for values of the smeared charge fraction, f, between 0 and 0.25 and the cross excluded-volume parameter between values of 40 and 185 Å^3. See Figure 1 for the actual points in the f vs v_{AC} plane for which the free energy changes of mixing, ΔF_{mix}, were examined as a function of polyelectrolyte chain composition, x_C, for various values of the spherical surface radius, R. In the region far from the onset of thermodynamic instability, the system is too deep in the mixed state with zero curvature. Although increasing the curvature causes ΔF_{mix} to be increased, this change is not sufficient to induce phase separation at reasonably small radii. On the other hand, near the boundary, the two driving forces are nearly balanced. Yet this balance is not symmetric with regards to composition; meaning, depending upon the value of f, both the higher and lower curvature systems could show more favorable mixing across the range of compositions. Of course, the lower curvature systems always approach instability first; see Supporting Information for plots illustrating this trend. For these reasons, in the mixing dominant regime we found no evidence for lower critical-type phase separation.

Conclusions

The effect of surface curvature upon the phase behavior of the mixed brush case was elucidated. In the regime where phase separation occurs in the flat limit, the effect of curving the surface is to favor a mixed state. This is due to a reduction in the contribution of the polymer–polymer cross excluded-volume interaction resulting from the spatial dilution of the curved geometry. However, in the regime where the electrostatic and excluded volume self-interactions are stronger than the cross excluded-volume contributions, less favorable mixed states can be found at higher curvature. This trend is, however, in general too weak to result in actual phase separation.

Acknowledgment. The authors are grateful for encouragement and support provided by Professor Sangtae Kim at Purdue University. We thank the American Chemical Society Petroleum Research Fund (Grant 46593-G7) and the Purdue Research Foundation Shreve Fund for supporting this research.

Supporting Information Available: Representative plots of free energy of mixing, ΔF_{mix}, as a function of polyelectrolyte chain composition, x_C, for various parameter conditions (Figures S1 and S2). This material is available free of charge via the Internet at http://pubs.acs.org.

References and Notes

(1) Halperin, A.; Tirrell, M.; Lodge, T. P. *Adv. Polym. Sci.* **1992**, *100*, 31–71.
(2) Naji, A.; Seidel, C.; Netz, R. R. *Adv. Polym. Sci.* **2006**, *198*, 149–183.

(3) Ruhe, J.; Ballauff, M.; Biesalski, M.; Dziezok, P.; Grohn, F.; Johannsmann, D.; Houbenov, N.; Hugenberg, N.; Konradi, R.; Minko, S.; Motornov, M.; Netz, R. R.; Schmidt, M.; Seidel, C.; Stamm, M.; Stephan, T.; Usov, D.; Zhang, H. N. *Adv. Polym. Sci.* **2004**, *165*, 79–150.
(4) Milner, S. T. *Science* **1991**, *251*, 905–914.
(5) Daoud, M.; Cotton, J. P. *J. Phys. (Paris)* **1982**, *43*, 531–538.
(6) Pincus, P. *Macromolecules* **1991**, *24*, 2912–2919.
(7) Biver, C.; Hariharan, R.; Mays, J.; Russel, W. B. *Macromolecules* **1997**, *30*, 1787–1792.
(8) Zhulina, E. B.; Birshtein, T. M.; Borisov, O. V. *Eur. Phys. J. E* **2006**, *20*, 243–256.
(9) Carignano, M. A.; Szleifer, I. *J. Chem. Phys.* **1995**, *102*, 8662–8669.
(10) Nap, R.; Gong, P.; Szleifer, I. *J. Polym. Sci., Part B: Polym. Phys.* **2006**, *44*, 2638–2662.
(11) Wijmans, C. M.; Zhulina, E. B. *Macromolecules* **1993**, *26*, 7214–7224.
(12) Dan, N.; Tirrell, M. *Macromolecules* **1992**, *25*, 2890–2895.
(13) Grest, G. S.; Kremer, K.; Witten, T. A. *Macromolecules* **1987**, *20*, 1376–1383.
(14) Murat, M.; Grest, G. S. *Macromolecules* **1991**, *24*, 704–708.
(15) Luzinov, I.; Minko, S.; Tsukruk, V. V. *Prog. Polym. Sci.* **2004**, *29*, 635–698.
(16) Minko, S. *Polym. Rev.* **2006**, *46*, 397–420.
(17) Zhou, F.; Huck, W. T. S. *Phys. Chem. Chem. Phys.* **2006**, *8*, 3815–3823.
(18) Dan, N.; Safran, S. A. *Macromolecules* **1994**, *27*, 5766–5772.
(19) Dan, N.; Tirrell, M. *Macromolecules* **1993**, *26*, 4310–4315.
(20) Sidorenko, A.; Minko, S.; Schenk-Meuser, K.; Duschner, H.; Stamm, M. *Langmuir* **1999**, *15*, 8349–8355.
(21) Marko, J. F.; Witten, T. A. *Phys. Rev. Lett.* **1991**, *66*, 1541–1544.
(22) Minko, S.; Muller, M.; Usov, D.; Scholl, A.; Froeck, C.; Stamm, M. *Phys. Rev. Lett.* **2002**, *88*, 035502.
(23) Muller, M. *Phys. Rev. E* **2002**, *65*, 030802.
(24) de Gennes, P. G. *Scaling Concepts in Polymer Physics*; Cornell University Press: Ithaca, NY, 1988.
(25) Halperin, A. *Europhys. Lett.* **1987**, *4*, 439–445.
(26) Witte, K. N.; Won, Y. Y. *Macromolecules* **2006**, *39*, 7757–7768.
(27) Khokhlov, A. R.; Nyrkova, I. A. *Macromolecules* **1992**, *25*, 1493–1502.
(28) Rabin, Y.; Marko, J. F. *Macromolecules* **1991**, *24*, 2134–2136.

MA071682E